Journal of Earth Science, *Vol. 27*, *No. 3*, *p. 391–402*, *June 2016* *ISSN 1674-487X*
Printed in China
DOI: 10.1007/s12583-016-0671-y

Geochemistry, Zircon U-Pb Age and Hf Isotopic Constraints on the Petrogenesis of the Silurian Rhyolites in the Loei Fold Belt and Their Tectonic Implications

Tianyu Zhao, **Xin Qian**, **Qinglai Feng***
State Key Laboratory of Geological Processes and Mineral Resources, *China University of Geosciences*, *Wuhan* 430074, *China*;
School of Earth Sciences, *China University of Geosciences*, *Wuhan* 430074, *China*

ABSTRACT: Zircon U-Pb dating, Lu-Hf isotopic and geochemical data for the Silurian rhyolites from the Loei fold belt are presented to constrain their petrogenesis and tectonic settings. The rhyolites give a weighted mean $^{206}Pb/^{238}U$ age of 423.7±2.7 Ma, and are characterized by high SiO_2, Al_2O_3, K_2O and low MnO, MgO and P_2O_5. All samples are enriched in LILEs (e.g., Ba, K, Pb) and LREEs and depleted in HFSEs (e.g., Nb, Ta, Ti) with obvious negative Eu-anomalies (δEu=0.56–0.63). The calc-alkaline rhyolites are typical arc-related rocks. The Loei rhyolites have high A/CNK ratios (1.19–1.34) and positive $\varepsilon_{Hf}(t)$ (4.03–5.38), which can be interpreted as partial melting of juvenile crustal materials followed by multistage melting and differentiation, similar to highly fractional I-type rocks. Combined with regional geological surveys, the Loei rhyolites should be formed in a volcanic arc environment and may be in contact with the Truong Son fold belt during the Early Paleozoic. Moreover, the Simao Block might be in contiguity with the Indochina Block during Silurian.

KEY WORDS: **I-type rhyolite, zircon U-Pb dating, Hf isotopic composition, geochemical characteristics, Loei fold belt; Indochina Block.**

0 INTRODUCTION

The Early Paleozoic was significant for the tectonic evolution of the Gondwana, in combination with the time of the collage of various terranes/blocks and subduction zones along the margin of Gondwana (Zhu et al., 2012). Thailand and its adjacent area comprises numerous terranes/blocks, including South China, Simao, Indochina, Sibumasu, Sukhothai, etc. (Fig. 1). These terranes/blocks are separated by several volcanic belts, including Loei fold belt, Truong Son fold belt, Nan suture and Chiang Mai suture, etc. (Fig. 1) (Qian et al., 2015; Panjasawatwong et al., 2006). The tectonic settings of these volcanic belts are hotly debated. Volcanic rocks play an essential role in flourishing tectonic evolution and mineral resources. The western margin of the Indochina Block may contain multiple suture zones including the Nan suture and Loei fold belt (Fig. 1) (Chonglakmani and Helmcke, 2001). The Loei fold belt has been intensely studied regarding the controversy over its regional tectonic evolution (Vivatpinyo et al., 2014; Udchachon et al., 2011; Panjasawatwong et al., 2006; Intasopa and Dunn, 1994). The volcanic rocks in the Loei fold belt can be separated into eastern, central and western sub-belts (Boonsoong et al., 2011; Panjasawatwong et al., 2006) (Fig. 2). The volcanic rocks of the eastern sub-belt are mainly rhyolitic rocks. The central sub-belt is composed mainly of pillow basalts and hyaloclastites (Udchachon et al., 2011; Khositanont et al., 2008; Intasopa and Dunn, 1994). The western sub-belt is dominated by andesites which have been interpreted as products of arc volcanism active during the the Permo–Triassic; volcanic rocks are also found in the Phetchabun belt, which is the southern extension of the western Loei sub-belt (Kamvong et al., 2014; Salam et al., 2014; Boonsoong et al., 2011; Panjasawatwong et al., 2006; Intasopa and Dunn, 1994; Jungyusuk and Khositanont, 1992; Bunopas and Vella, 1983). Intasopa and Dunn (1994) firstly suggested that these rhyolites formed in an arc setting during the subduction of the Cathaysia Block and yielded a whole-rock Rb-Sr isochron age of 374±33 Ma (Late Devonian). Khositanont et al. (2008) reported U-Pb zircon ages of 425±7 and 433±4 Ma (Early Silurian) for the volcaniclastics in the eastern sub-belt. However, the tectonic evolution and magmatic processes of rhyolites in the eastern Loei sub-belt have been poorly studied and its northern extension is still debated.

Because of these different views and problems, we carried out a geological survey in the Loei fold belt. The purposes of this paper are to present a new LA-ICP-MS U-Pb zircon age, zircon Hf isotopic compositions and geochemical data of the rhyolites from the eastern sub-belt in northeastern (NE) Thailand. The aims of this study include: (1) to constrain the formation time and geochemical characteristics of the rhyolites;

*Corresponding author: qinglaifeng@cug.edu.cn

Manuscript received June 11, 2015.
Manuscript accepted December 12, 2015.

Zhao, T. Y., Qian, X., Feng, Q. L., 2016. Geochemistry, Zircon U-Pb Age and Hf Isotopic Constraints on the Petrogenesis of the Silurian Rhyolites in the Loei Fold Belt and Their Tectonic Implications. *Journal of Earth Science*, 27(3): 391–402. doi:10.1007/s12583-016-0671-y. http://en.earth-science.net

(2) to probe into the origin and petrogenesis of the rhyolites; (3) discuss their tectonic setting.

1 GEOLOGICAL BACKGROUND

The study area is located in the northeastern portion of the folded mountain range west of the Khorate Plateau (Fig. 1). The oldest rocks are Silurian volcanic rocks, including rhyolites, andesites and tuffs, which outcrop in the eastern part of the Loei area. They are in fault contact with Carboniferous rocks. The Silurian to Devonian sedimentary rocks consist of shales, fine-grained tuffaceous, sandstones and siltstones. They are exposed along the eastern map area (Fig. 2). The Carboniferous sedimentary rocks are mainly shales and reef limestones. The volcanic rocks are divided into three sub-belts along the eastern, western and central parts of the Loei area. They are Silurian, Devonian–Carboniferous and Permo–Triassic. The volcanic rocks of western sub-belt are mainly granites and rhyolites. They are products of volcanism along an active continental margin during Permian–Triassic time (Boonsoong et al., 2011; Khositanont et al., 2008). The central sub-belt involves the Late Devonian–Early Carboniferous pillow lava, hyaloclastite, and pillow breccia (Panjasawatwongg et al., 2006). The eastern sub-belt rocks show poor relations to the other rocks, including rhyolites, andesite and volcaniclastic rocks. This paper concentrates on the rhyolites of the eastern sub-belt (Fig. 2).

Five fresh samples were selected from the eastern Loei sub-belt in NE Thailand (18°9.910′N, 102°10.508′E). They are fine-grained rhyolites with porphyritic texture, the main phenocryst phases (30 wt.%–40 wt.%) of which are quartz, sanidine and plagioclase. Crystal sizes vary from 0.5 to 4 mm. Quartz phenocrysts show dissolution textures. Plagioclases are subhedral to euhedral with sizes ranging from 0.5 to 2 mm. The groundmass is principally felsitic and microspherulitic.

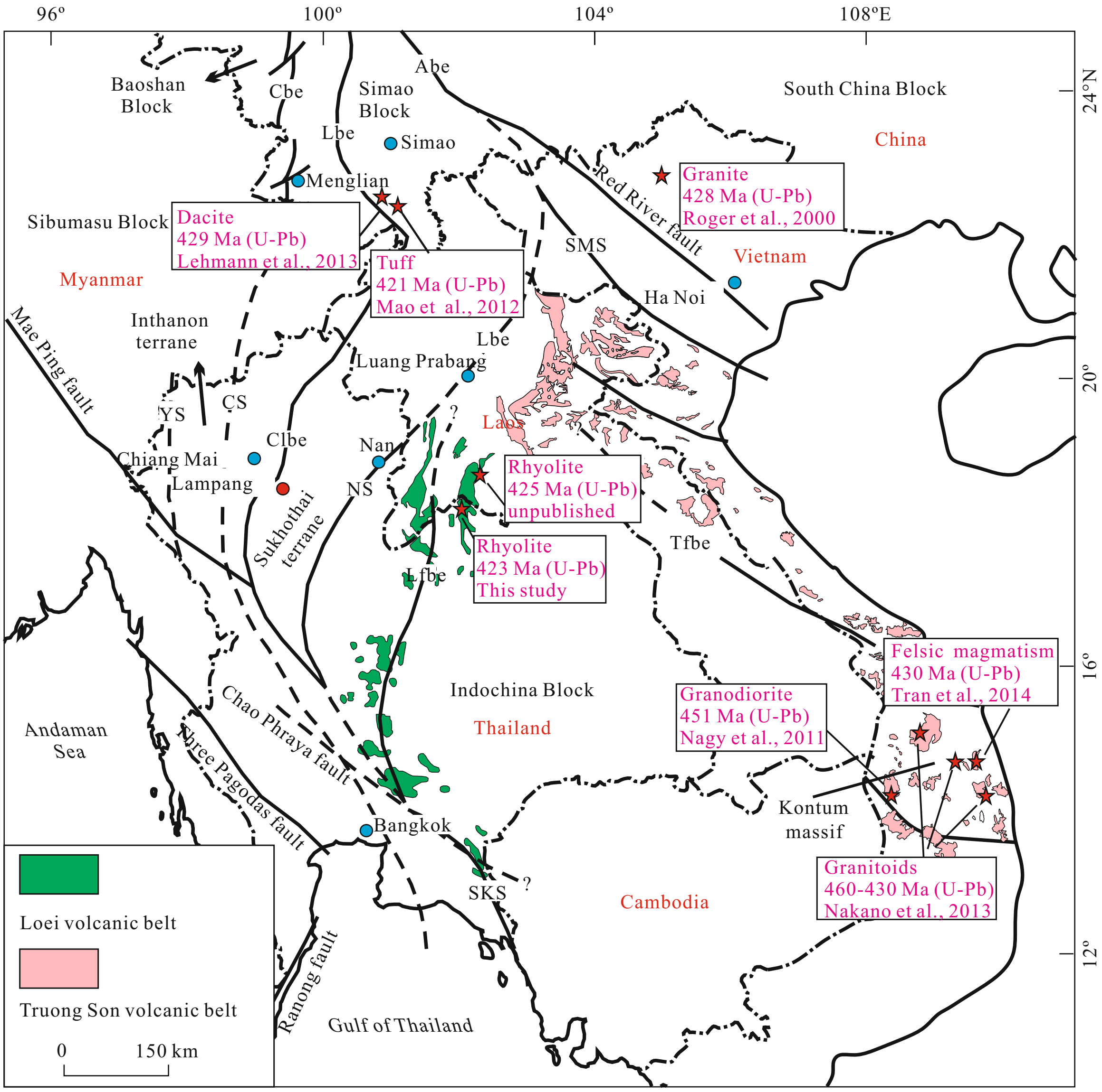

Figure 1. Skeptically tectonic map (revised after Qian et al., 2015, 2013; Barr et al., 2006; Feng et al., 2005). Abe (AB). Ailaoshan belt; Lbe (LB). Lancangjiang belt; Cbe (CMB). Changning-Menglian belt; SMS. Song Ma suture; Tfbe. Truong Son fold belt; Lfbe (LFB). Loei fold belt; Lbe (LB). Luang Prabang belt; SKS. Sa Kaew suture; NS. Nan suture; Clbe. Chiang Kong-Lampang-Tak belt; CS. Chiang Mai suture; YS. Yuam suture.

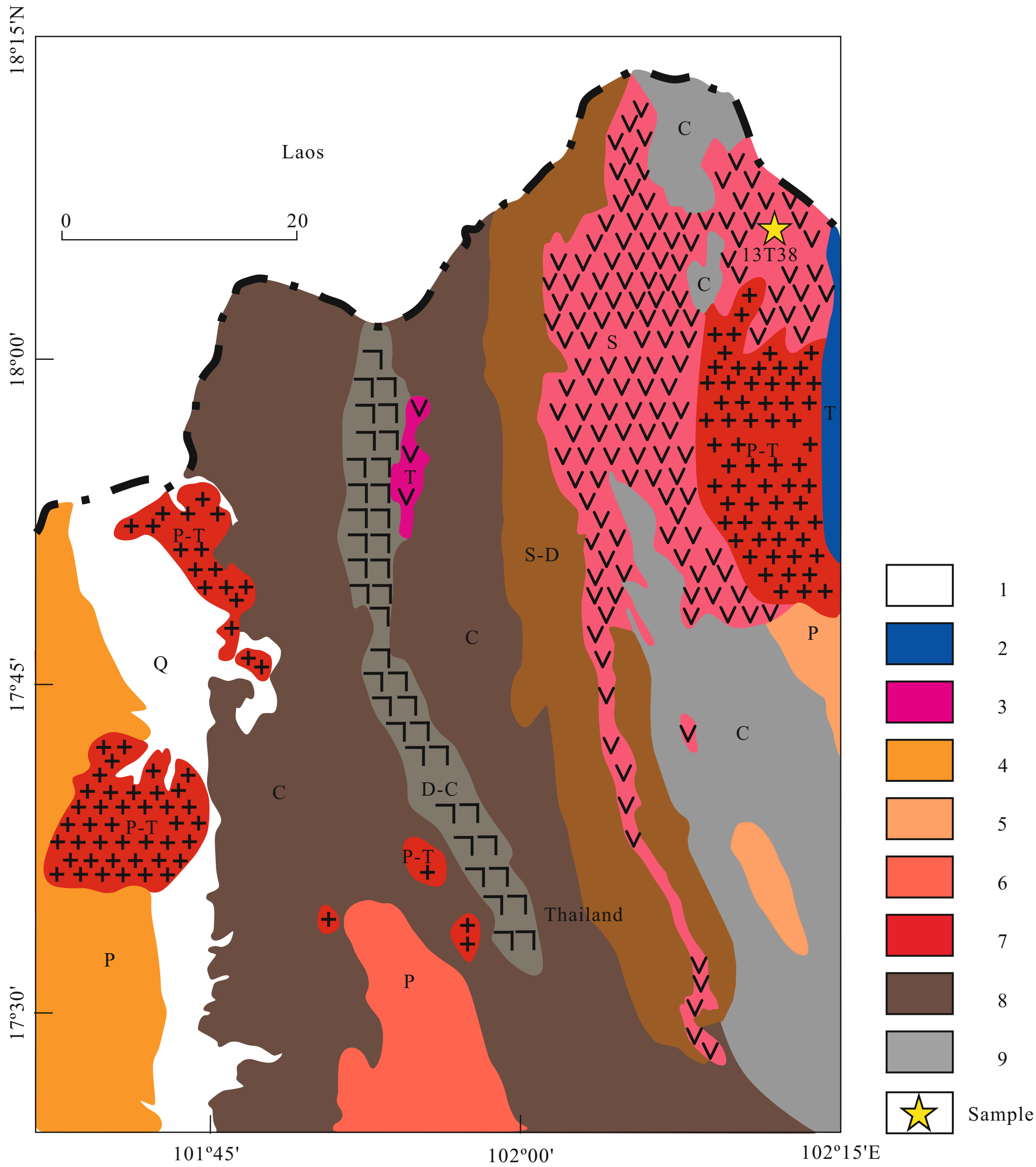

Figure 2. Simplified geological map of Loei showing distribution of sedimentary sequences and volcanic rocks. 1. Quaternary rock; 2. Trassic sedimentary rock; 3. Trassic volcanic rock; 4. Permian sedimentary rock; 5. Permo–Trassic granite; 6. Carboniferous sedimentary rock; 7. Devono–Carboniferous volcanic rock; 8. Silurian–Devonian sedimentary rock; 9. Silurian volcanic rock (revised after Udchachon et al., 2011; Charoenprawat et al., 1976).

2 ANALYTICAL METHODS

2.1 LA-ICP-MS Zircon U-Pb Dating and Hf-Isotope Analyses

Zircons from sample 13T38 were separated by standard heavy liquid and magnetic techniques, mounted in epoxy and then polished. The zircon grains CL images for observing internal structures were accomplished by JEOL JXA-8100 electron microscope. Zircon U-Pb dating was performed on LA-ICP-MS at the State Key Laboratory of Geological Processes and Mineral Resources (GPMR), China University of Geosciences, Wuhan. Detailed analytical procedure followed Liu et al. (2010). Laser sampling was conducted using a GeoLas 2005 system and ion-signal intensities were performed by Agilent 7500a ICP-MS. The spot size was 32 μm, with each analysis including a background gathering of around 20 and 50 s of data acquisition from the samples. Off-line selection and integration of background and analyte signals, and time-drift correction and quantitative calibration for U-Pb dating were performed using ICPMSDataCal (Liu et al., 2009). External standard zircon 91500 was used as primary reference material for U-Pb dating. Concordia diagrams and weighted mean calculations were made using Isoplot/Ex_ver3 (Ludwig, 2003). The analytical results for the samples are shown in Table 1.

Lu-Hf isotope experiments were carried out using a Neptune Plus MC-ICP-MS (Thermo Fisher Scientific, Germany) in combination with a Geolas 2005 excimer ArF laser ablation system (Lambda Physik, Göttingen, Germany) that was hosted at GPMR, China University of Geosciences in Wuhan. The single spot diameter is 44 μm for all zircon grains. The 91500 zircon standard was used for calibration. Detailed operating conditions for the laser ablation system and the MC-ICP-MS instrument and analytical method followed Hu et al. (2012). Off-line selection and integration of analyte signals, and mass bias calibrations were performed using ICPMSDataCal (Liu et al., 2009). The analytical results for the samples are shown in Table 2.

2.2 Whole Rock Major and Trace Elements

Major elements were analyzed by X-ray fluorescence (XRF) method at the State Key Laboratory of Geological Processes and Mineral Resources, China University of Geosciences in Wuhan, the analysis precision is generally better than 5 wt.%. Whole rock samples were crushed in a corundum jaw crusher (to 60 meshes). About 60 g was powdered in an agate ring mill to less than 200 meshes. The samples were then digested by $HF+HNO_3$ in Teflon bombs and analyzed with an Agilent 7500a ICP-MS at the GPMR. The detailed sample-digesting procedure for ICP-MS analyses and analytical precision and accuracy for trace elements are the same as description by (Liu et al., 2008). The analytical results for the samples are shown in Table 3.

Table 1 LA-ICP-MS zircon U-Pb data for the rhyolites in the Loei fold belt

Spot No.	Concentration		Th/U	Isotope ratio						Calculated apparent age (Ma)					
	Th	U		^{207}Pb/^{206}Pb		^{207}Pb/^{235}U		^{206}Pb/^{238}U		^{207}Pb/^{206}Pb		^{207}Pb/^{235}U		^{206}Pb/^{238}U	
	(ppm)			Ratio	±1σ	Ratio	±1σ	Ratio	±1σ	Age	±1σ	Age	±1σ	Age	±1σ
13T38-1	285	521	0.55	0.056 3	0.002 5	0.534 6	0.024 2	0.068 4	0.000 8	465	98	435	16	427	5
13T38-3	559	1 077	0.52	0.057 9	0.002 1	0.538 2	0.019 3	0.067 0	0.000 7	528	75	437	13	418	4
13T38-4	449	886	0.51	0.058 0	0.002 2	0.539 6	0.020 0	0.067 2	0.000 8	528	82	438	13	419	5
13T38-5	246	478	0.52	0.057 7	0.003 0	0.532 9	0.028 4	0.066 4	0.000 8	517	115	434	19	414	5
13T38-6	868	1 298	0.67	0.056 5	0.001 9	0.537 5	0.017 9	0.068 3	0.000 7	478	74	437	12	426	4
13T38-7	433	635	0.68	0.049 1	0.003 3	0.455 6	0.028 9	0.067 8	0.001 2	154	152	381	20	423	7
13T38-8	469	1 071	0.44	0.055 3	0.001 9	0.538 0	0.018 7	0.070 0	0.000 7	433	76	437	12	436	4
13T38-9	679	1 004	0.68	0.055 2	0.00 2 0	0.519 8	0.018 6	0.068 1	0.000 8	420	77	425	12	425	5
13T38-10	271	585	0.46	0.055 1	0.002 3	0.518 7	0.021 5	0.068 4	0.000 8	417	94	424	14	426	5
13T38-12	517	917	0.56	0.056 7	0.001 9	0.537 2	0.017 5	0.068 9	0.000 7	480	44	437	12	430	4
13T38-13	446	951	0.47	0.055 8	0.001 8	0.524 8	0.015 9	0.068 7	0.000 8	443	75	428	11	428	5
13T38-14	452	749	0.6	0.055 1	0.002 2	0.512 1	0.020 0	0.067 5	0.000 7	417	89	420	13	421	4
13T38-15	235	464	0.51	0.059 0	0.002 9	0.556 2	0.028 3	0.067 9	0.000 9	569	138	449	18	423	5
13T38-16	355	690	0.51	0.053 7	0.002 3	0.506 3	0.020 4	0.068 7	0.000 9	361	96	416	14	428	5
13T38-17	333	577	0.58	0.055 1	0.002 2	0.515 4	0.020 2	0.068 3	0.001 0	417	93	422	14	426	6
13T38-18	497	1 136	0.44	0.053 2	0.002 0	0.489 6	0.017 7	0.066 8	0.000 9	339	85	405	12	417	5
13T38-19	260	515	0.5	0.050 1	0.002 5	0.465 1	0.022 5	0.067 6	0.000 9	198	115	388	16	422	5
13T38-20	474	743	0.64	0.053 1	0.002 3	0.492 1	0.021 6	0.066 7	0.001 0	332	101	406	15	416	6
13T38-22	597	1 050	0.57	0.052 5	0.002 4	0.492 6	0.022 3	0.067 9	0.000 8	306	107	407	15	423	5
13T38-23	497	1 157	0.43	0.055 2	0.002 0	0.504 0	0.018 0	0.066 0	0.000 8	420	80	414	12	412	5
13T38-24	1 315	2 324	0.57	0.053 7	0.001 6	0.511 5	0.015 0	0.068 9	0.000 7	367	73	419	10	429	4

Table 2 Zircon in-situ Lu-Hf isotopic compositions of the rhyolites in the Loei fold belt

Spot No.	Age (Ma)	^{176}Hf/^{77}Hf	±1σ	^{176}Lu/^{177}Hf	±1σ	^{176}Yb/^{177}Hf	±1σ	T_{1DM} (Ma)	T_{2DM} (Ma)	$\varepsilon_{Hf}(t)$
13T38-1	427	0.282 662	0.000 011	0.001 356	0.000 020	0.043 524	0.000 994	844	1 003	5.11
13T38-3	418	0.282 671	0.000 016	0.002 819	0.000 055	0.082 792	0.001 539	865	1 011	4.84
13T38-4	419	0.282 652	0.000 014	0.001 378	0.000 034	0.044 657	0.001 487	858	1 025	4.61
13T38-7	423	0.282 683	0.000 017	0.002 832	0.000 085	0.094 734	0.002 881	847	985	5.38
13T38-13	428	0.282 656	0.000 010	0.001 277	0.000 011	0.040 993	0.000 323	850	1 013	4.96
13T38-14	421	0.282 645	0.000 011	0.001 049	0.000 011	0.035 754	0.000 302	861	1 033	4.49
13T38-15	423	0.282 644	0.000 013	0.001 098	0.000 008	0.042 530	0.000 686	863	1 035	4.49
13T38-16	428	0.282 631	0.000 014	0.001 274	0.000 012	0.047 696	0.000 563	885	1 061	4.09
13T38-18	417	0.282 647	0.000 013	0.001 143	0.000 014	0.041 932	0.000 764	859	1 032	4.46
13T38-22	423	0.282 652	0.000 013	0.001 743	0.000 044	0.064 172	0.001 461	866	1 029	4.59
13T38-24	429	0.282 638	0.000 017	0.002 369	0.000 078	0.074 833	0.001 537	902	1 065	4.03
13T38-20	416	0.282 654	0.000 015	0.001 397	0.000 005	0.052 997	0.000 546	855	1 022	4.61

Table 3 Major and trace elements analytical data for the rhyolites in the Loei fold belt

Sample	13T38-1	13T38-2	13T38-3	13T38-4	13T38-5
Major oxide (wt.%)					
SiO_2	77.00	76.78	76.47	76.91	75.61
TiO_2	0.22	0.21	0.21	0.24	0.23
Al_2O_3	12.10	12.71	12.72	12.67	13.13
FeOt	2.20	2.21	2.20	0.98	2.24
MnO	0.07	0.07	0.07	0.03	0.07
MgO	0.38	0.51	0.51	0.24	0.44
CaO	0.50	0.38	0.37	0.26	0.61
Na_2O	3.64	3.13	3.27	3.74	3.63
K_2O	2.97	3.39	3.44	3.25	3.50
P_2O_5	0.04	0.04	0.05	0.03	0.06
LOI	0.87	1.23	1.15	1.07	1.00
Total	99.99	100.66	100.46	99.42	100.52
A/CNK	1.20	1.34	1.30	1.25	1.21
Na_2O+K_2O	6.62	6.52	6.72	7.00	7.13
Na_2O/K_2O	0.82	0.87	0.96	1.05	1.08
Mg#	26.00	31.00	31.00	32.00	28.00
Trace element (ppm)					
La	28.44	22.55	21.88	55.96	28.89
Ce	54.17	45.85	45.52	90.53	54.50
Pr	6.57	5.74	5.78	13.10	6.64
Nd	24.60	21.37	21.77	48.60	24.18
Sm	5.06	4.53	4.57	10.22	4.84
Eu	0.91	0.89	0.86	1.94	0.87
Gd	4.47	4.20	4.41	9.70	4.57
Tb	0.79	0.78	0.80	1.73	0.82
Dy	4.71	4.69	4.78	9.87	4.96
Ho	0.98	1.00	1.02	1.92	1.03
Er	3.11	3.11	3.16	5.31	3.16
Tm	0.54	0.53	0.55	0.87	0.55
Yb	3.23	3.14	3.20	4.96	3.26
Lu	0.51	0.49	0.49	0.70	0.49
Y	30.34	29.18	31.28	51.86	31.88
Li	17.02	24.24	23.79	7.58	19.97
Be	1.37	1.58	1.46	1.38	1.71
Sc	8.91	7.73	8.74	8.97	8.62
Co	69.00	58.01	58.58	54.50	72.44
Cu	0.94	0.35	0.22	0.55	0.47
Zn	33.91	49.89	50.53	27.87	35.33
Ga	10.71	14.21	14.02	12.94	13.69
Rb	68.80	81.97	82.83	88.77	84.88
Zr	134.90	133.50	131.90	144.50	142.50
Nb	7.67	7.60	8.95	10.16	8.47
Mo	0.10	0.08	0.08	0.13	0.09
Cs	2.58	3.64	3.81	2.74	2.69
Hf	4.68	4.67	4.72	5.03	4.97
Ta	0.82	0.80	0.79	0.86	0.91
Pb	8.10	7.85	8.48	7.81	8.01
Th	7.86	7.40	7.03	6.68	6.02
U	2.47	2.55	2.68	2.53	2.39
Sn	2.04	2.33	2.43	2.34	2.52
Ba	908.99	1 431.28	1 427.61	1 340.43	1 385.20
Cr	7.40	7.22	7.22	4.14	7.68
Ni	2.90	2.63	2.34	2.15	3.26

Table 3 Continued

Sample	13T38-1	13T38-2	13T38-3	13T38-4	13T38-5
Trace element (ppm)					
Sr	144.32	154.32	148.45	186.63	209.56
V	8.50	8.90	8.50	7.44	9.12
∑REE	138.08	118.85	118.79	255.41	138.76
$(La/Yb)_N$	4.60	4.84	5.94	5.97	7.61
δEu	0.63	0.60	0.59	0.58	0.56
Tzr (°C)	791.30	799.10	795.50	800.50	795.00
CIPW (%)					
Q	42.94	44.16	42.86	41.93	39.30
C	2.10	3.33	3.06	2.65	2.40
Or	17.58	20.03	20.35	19.21	20.69
Ab	30.81	26.51	27.69	31.68	30.70
An	2.14	1.53	1.50	0.96	2.66
Hy	0.95	1.27	1.26	0.59	1.09
Il	0.15	0.15	0.15	0.06	0.15
Ru	0.14	0.13	0.13	0.20	0.15
Ap	0.12	0.12	0.13	0.12	0.13
Sum	96.94	97.23	97.12	97.39	97.27
DI	91.33	90.70	90.90	92.82	90.69

FeOt represents total Fe-oxides; Mg#=molar Mg×100/(Mg+Fe); LOI. loss on ignition; A/CNK=molar $Al_2O_3/(CaO+Na_2O+K_2O)$; DI=Q+Or+Ab.

3 RESULTS

3.1 Zircon U-Pb Geochronology and Lu-Hf Isotopic Compositions

The zircon grains of sample are mainly euhedral and exhibit a prismatic crystal form with oscillatory magmatic zoning in CL images, ranging in length/width ratios of 3 : 1–3 : 2 (Fig. 3a). Twenty-one analyzed zircons have varying U (464 ppm–2 324 ppm) and Th (235 ppm–1 315 ppm) contents with Th/U ratios ranging from 0.43 to 0.68, in conformity with a magmatic origin (Hoskin and Schaltegger, 2003). Twenty-one analyses are concordant and yield a weighted mean $^{206}Pb/^{238}U$ age of 423.7±2.7 Ma (MSWD=1.5, n=21 (Figs. 3b, 3c).

Twelve dated zircon grains from samples 13T38 were analyzed for Lu-Hf isotope ratios (Table 2). Their $^{176}Hf/^{177}Hf$ values vary from 0.282 631 to 0.282 683. The $^{176}Lu/^{177}Hf$ ratios range from 0.001 049 to 0.002 832, indicating a low radiogenic growth of ^{176}Hf. Samples have positive $\varepsilon_{Hf}(t)$ values of 4.03 to 5.38 (average=4.63) and two-stage model age (T_{2DM}) range from 985 to 1 065 Ma (Table 2, Fig. 4), suggesting an origin from a juvenile crust.

3.2 Major and Trace Elements

The Loei rhyolites show high SiO_2 (75 wt.%–77 wt.%), Al_2O_3 (12.10 wt.%–13.13 wt.%), K_2O (2.97 wt.%–3.50 wt.%) and low MgO (0.24 wt.%–0.51 wt.%) and P_2O_5 (0.03 wt.%–0.06 wt.%). The K_2O+Na_2O values vary between 6.61 wt.% and 7.12 wt.%. The molecular A/CNK (molar $Al_2O_3/(CaO+Na_2O+K_2O)$ ratios of the samples range from 1.19 to 1.34, classified as characteristics of strongly peraluminous (Fig. 5a) (Maniar and Piccoli, 1989). The differentiation index (DI) varies between 90.70 and 92.82, suggesting that the magma

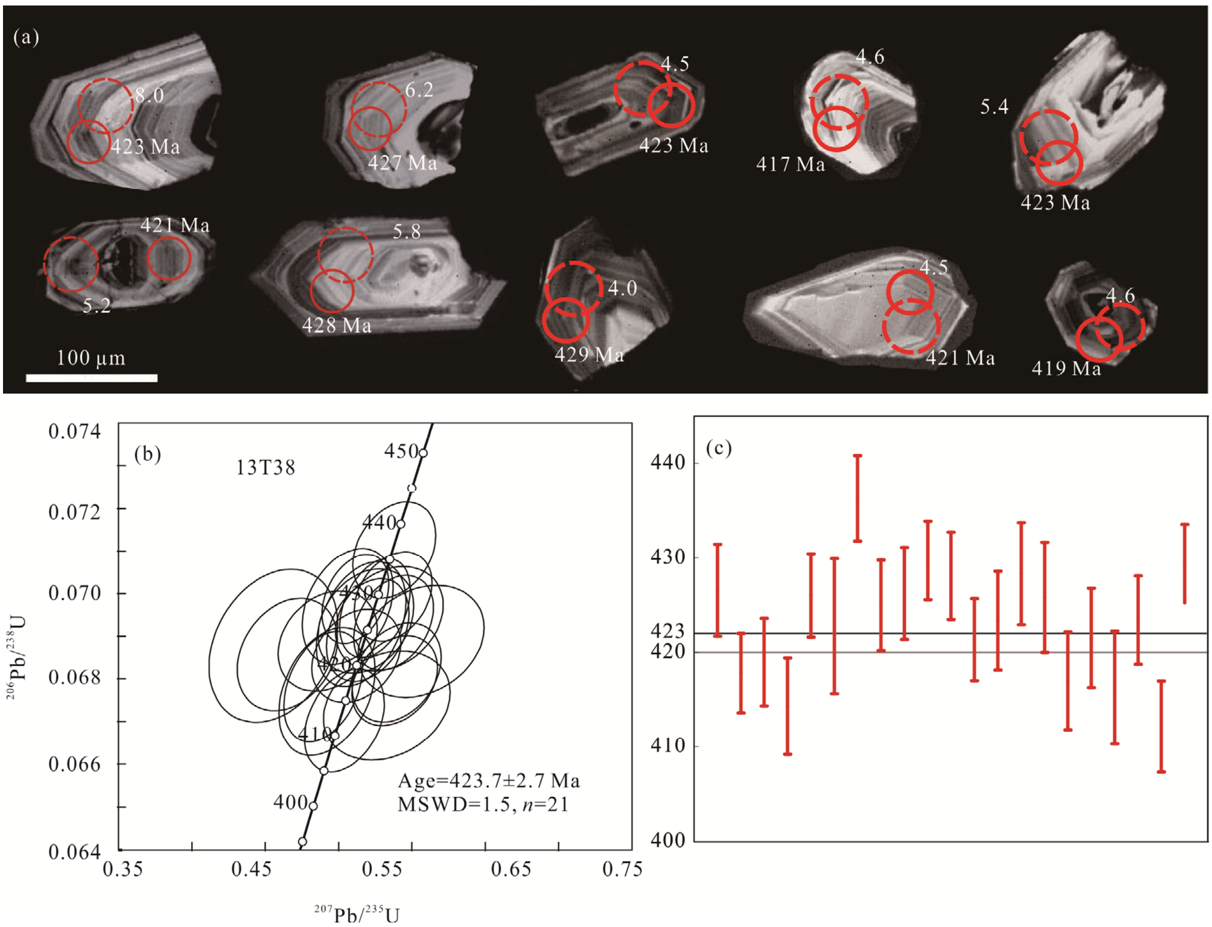

Figure 3. Representative CL images (a) and U-Pb concordia diagram (b) for the Loei rhyolites, (c) the solid line and dotted line circle on the analysed zircon grains show the positions of U-Pb analytical and Hf isotope sites, respectively.

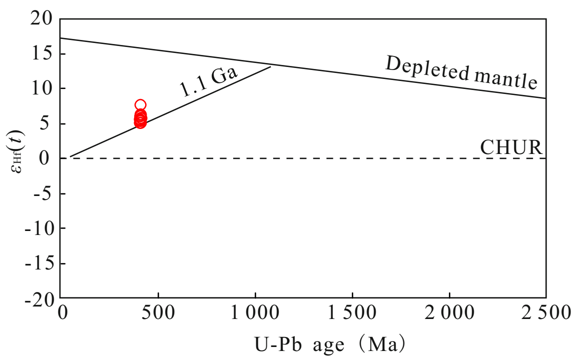

Figure 4. Plots of $\varepsilon_{Hf}(t)$ vs. U-Pb ages diagram.

was highly evolved. Samples plot within the field of calc-alkaline series on AFM diagram (Fig. 5c) (Irvine and Baragar, 1971). In the K_2O+Na_2O-SiO_2 and Zr/TiO_2-Nb/Y diagrams (Figs. 5b, 5d) (Le Bas et al., 1986; Winchester and Floyd, 1977), all samples plot in the field of rhyolite and rhyodacite/dacite.

In the primitive mantle-normalized multielement spidergram (Fig. 6a), all samples are enriched in large ion lithophile elements (LILEs) (e.g., Ba, K, Pb) and LREEs and depleted in high field-strength elements (HFSEs) (e.g., Nb, Ta, Ti). The total rare earth elements (∑REE) of the Loei rhyolites range from 118.79 ppm to 255.40 ppm (averaging 153.98 ppm). These samples display similar chondrite-normalized REE patterns (Fig. 6b). Samples have enriched LREEs with $(La/Yb)_N$ (N herein refers to chondrite-normalized value) ratios ranging from 4.60 to 7.61. The rhyolites show obvious negative Eu-anomalies (δEu=0.58–0.63). The calculated Zr saturation temperatures of the rhyolites range from 791 to 800 °C (Table 3).

4 DISCUSSION

4.1 Constrains on the Age of the Loei Rhyolites

The emplacement age of Loei rhyolites has been confusing because of its poor contacts with other stratigraphical well-defined rocks. Intasopa and Dunn (1994) reported a whole-rock Rb-Sr isochron age of 374±33 Ma (Late Devonian). Khositanont et al. (2008) reported U-Pb zircon ages of 425±7 and 433±4 Ma (Early Silurian) for the volcaniclastics in the eastern sub-belt. Our zircon grains from the rhyolites in the eastern sub-belt of Loei fold belt yield a weighted mean $^{206}Pb/^{238}U$ age of 423.7±2.7 Ma, indicating a Middle Silurian emplacement of the rhyolites. Detrital zircons from sedimentary rocks in the Loei area record a distinct age peak at ~425 Ma (Burrett et al., 2014). Consequently, we proposed a significant magmatism event which took place in the western margin of the Indochina Block during the Middle Silurian.

4.2 Petrogenesis of the Rhyolites

Our samples are fresh samples and they have low LOI. They show Zr correlating with Rb and Ba, suggesting that their

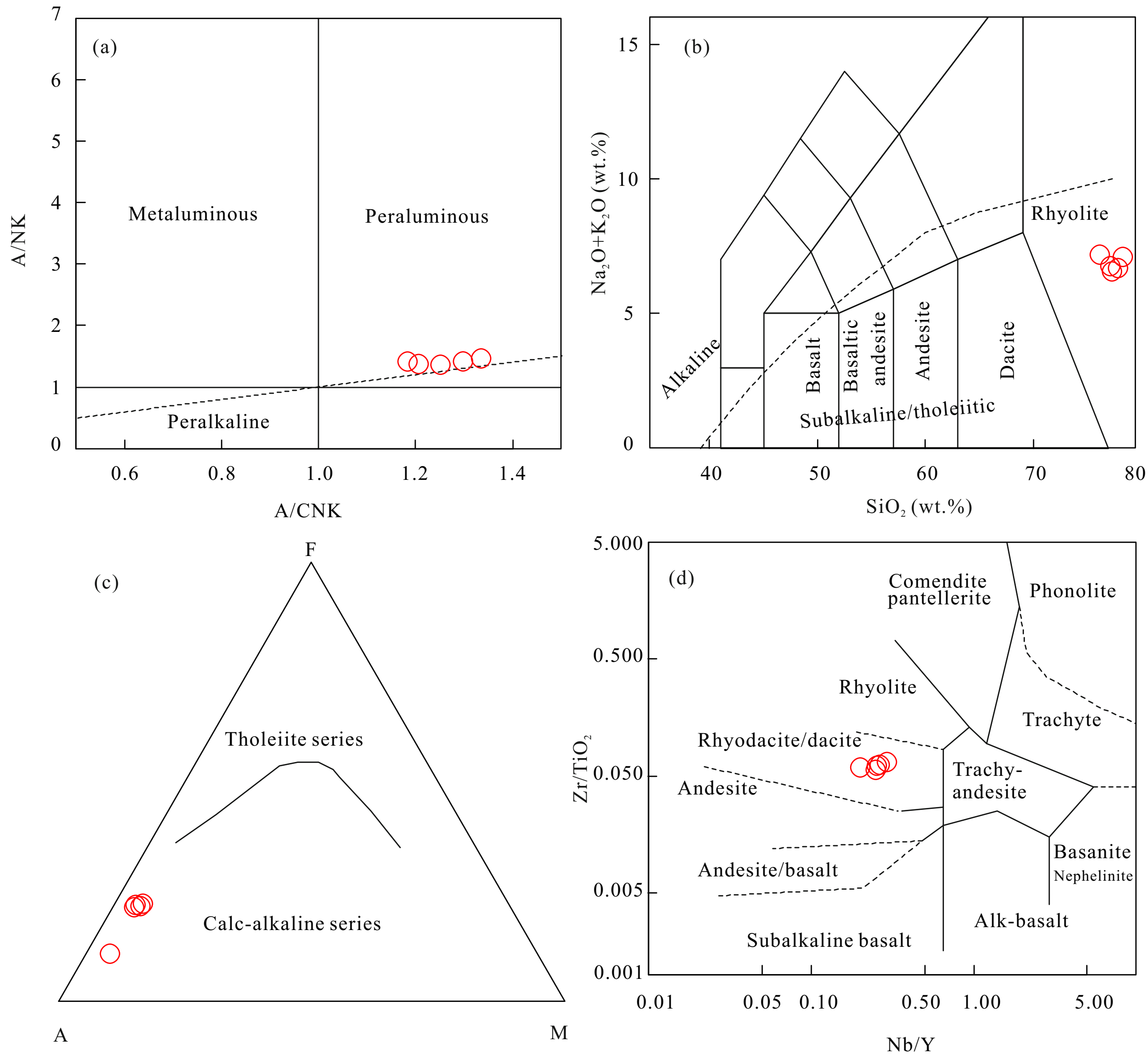

Figure 5. (a) A/CNK vs. A/NK relation diagram (after Maniar and Piccoli, 1989), (b) TAS diagram (after Le Bas et al., 1986), (c) AFM diagram (A=Na_2O+K_2O; M=MgO; F=FeOt) (after Irvine and Baragar, 1971), (d) Nb/Y vs. Zr/TiO_2 (after Winchester and Floyd, 1977).

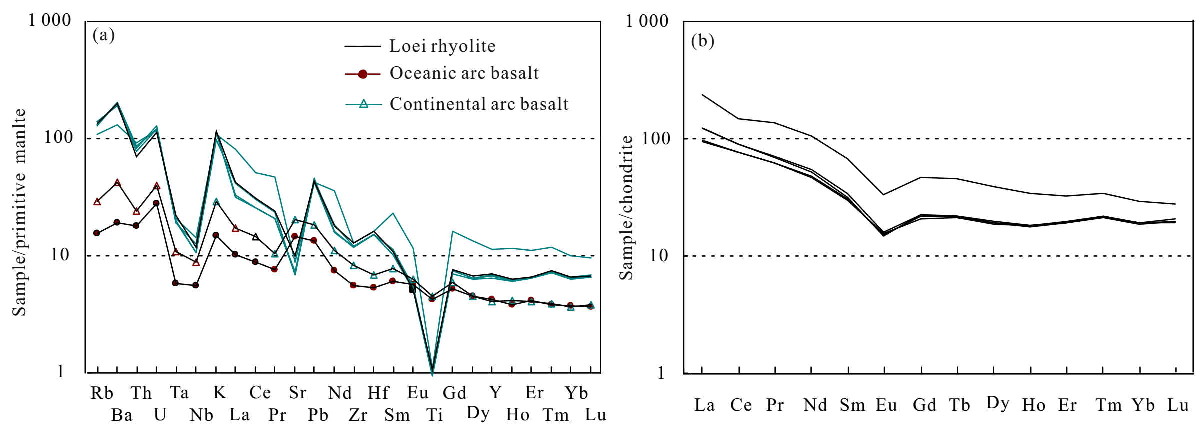

Figure 6. Primitive mantle-normalized trace-element patterns (a) and chondrite-normalized rare earth-element patterns (primitive mantle and chondrite values are from (Sun and McDonough, 1989) (b) for samples from Loei rhyolite. Continental arc and oceanic arc basalts are from (Kelemen et al., 2003).

mobility of LILEs (e.g., Rb, Sr and Ba) after eruption of the rocks does not seriously change their contents (Wang Q F et al., 2014), therefore most of the data/index are available.

The high SiO_2 (75 wt.%–77 wt.%), total alkali (K_2O+Na_2O =6.61 wt.%–7.12 wt.%), differentiation index of the Loei rhyolites samples (Table 3), suggest that the Loei rhyolites highly evolved. Although the high A/CNK values (1.20–1.34) resemble those of the S-type granites, however, different types of highly evoloved rocks (I-, S- and A-type) tend to have similar geochemical features, A/CNK will become increasingly for both I-type and S-type granitoids with sendimentary material involved or the process of fractional crystallization (Tao et al., 2013). Moreover, the positive $\varepsilon_{Hf}(t)$ of Loei rhyolites indicate that the protolith of Loei rhyolites were juvenile crust which is similar to the I-type granites. In the Rb/Sr-Rb/Ba diagram (Fig. 7) (Sylvester, 1998), all samples plot within the clay-poor area. Loei rhyolites also have high $\varepsilon_{Nd}(t)$ (-1.35–0.39) (Intasopa and Dunn, 1994), suggesting that they were from the reworking of juvenile crust rather than ancient materials.

P_2O_5 is an important feature to differentiate between the I-type granitoids and S-type granitoids because of apatite is soluble in peraluminous melt and P_2O_5 would soar with SiO_2 content during magmatic differentiation in S-type melts and decrease with SiO_2 in I-type (Li et al., 2007; Chappell, 1999). Samples show a decreasing trend of P_2O_5 contents with increasing SiO_2 (Fig. 8b). On the K_2O versus Na_2O diagram (Liu et al., 2014) (Fig. 8a), they also show I-type trend. Furthermore, in the FeOt/MgO and (Na_2O+K_2O)/CaO versus Zr+Nb+Ce+Y classification diagrams (Whalen et al., 1987), all samples plot within the field of Fractionated granites (Figs. 7c, 7d).

The geochemical features of Loei rhyolites are significantly different from the A-type granite: (1) the A-type granites are rich in HFSEs and depleted in Ba and Sr (Wu et al., 2003b; Whalen et al., 1987), whereas the Loei rhyolite show lower HFSEs and higher in Ba, Sr, (2) low FeOt/MgO (3.73–5.18) are different from the A-type granite (FeOt/MgO>10 (Whalen et al., 1987), (3) in the Nb, Zr, Na_2O+K_2O, K_2O/MgO-Ga/Al diagrams (Fig. 9) (Whalen et al., 1987), all samples plot outside the field of the A-types, this, combined with the relatively low petrogenetic temperatures (whole rocks Zr saturation temperatures: 791–800 °C), excludes the possibility of the A-type granitoids.

Loei rhyolites are depleted in Nb, Ta, Sr, P, Ti and Eu, therefore, primitive magma experienced fractional crystallizaiton. Depletions in Nb, Ta, and Ti commonly ascertain the

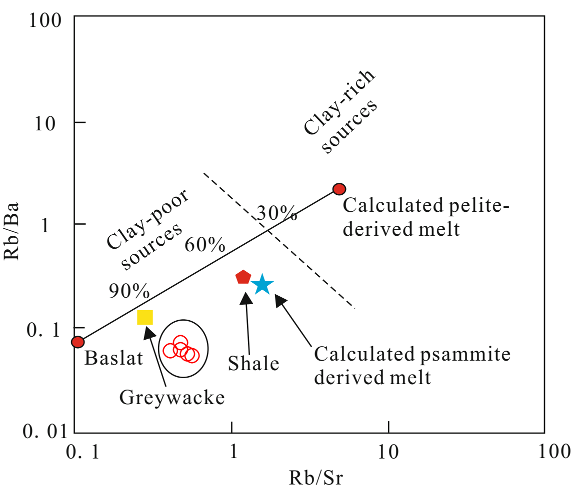

Figure 7. Rb/Ba vs. Rb/Sr diagram (after Sylvester, 1998).

fractionation of Ti-bearing phases. Apatite fractionation explains negative P concentration. Negative Eu and Sr manifest separation of plagioclase. Collectively, Loei rhyolites are highly evolved I-type rocks which have experienced extensive fractional crystallization.

Zircon Lu-Hf isotope is an effective geochemical tracer in protolith and petrogenesis (Zhao et al., 2014; Dong et al., 2013; Ji et al., 2009; Kinny and Maas, 2003). Magma derived from the mantle or juvenile crust has relatively higher $^{176}Lu/^{177}Hf$ and positive $\varepsilon_{Hf}(t)$ values, whereas low $^{176}Lu/^{177}Hf$ and negative $\varepsilon_{Hf}(t)$ values indicate derivation from ancient crust. Mixing of two end-members of juvenile crust and ancient crust, however, may produce varying $\varepsilon_{Hf}(t)$ values.

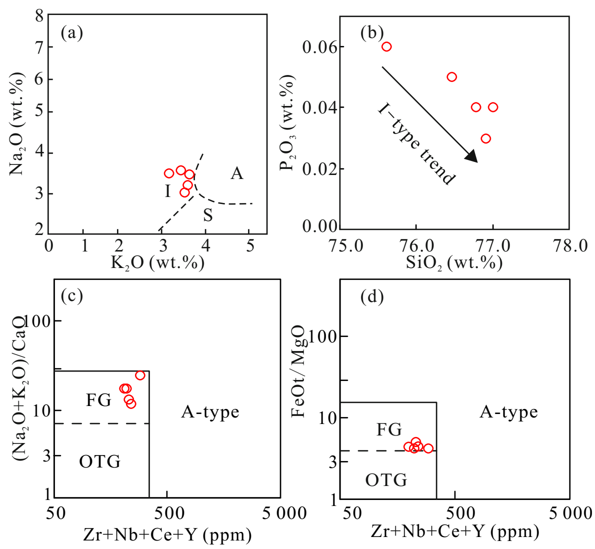

Figure 8. Selected geochemical diagrams of the Loei rhyolites. (a) K_2O vs. Na_2O (after Liu et al., 2014); (b) SiO_2 vs. P_2O_5; (c)–(d) FeOt/MgO and Na_2O+K_2O)/CaO vs. 10 000×Ga/Al classification diagram (after Whalen et al., 1987); FG. fractionated felsic granites; OGT. field for M-, I- and S-type granitoids.

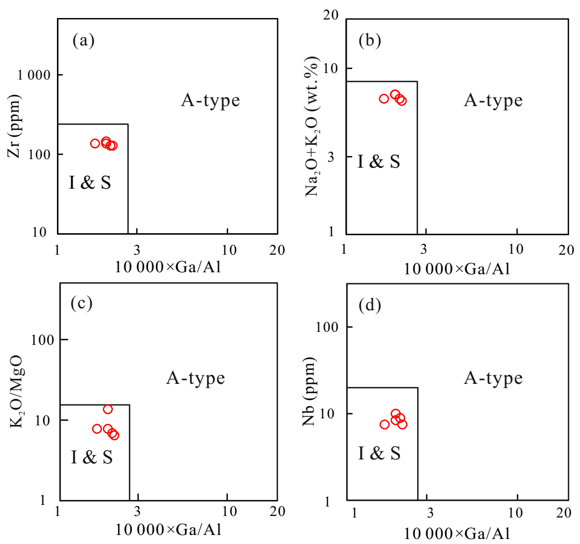

Figure 9. Plots of (a) Zr, (b) Na_2O+K_2O, (c) K_2O/MgO, (d) Nb vs. 1 000×Ga/Al (after Whalen et al., 1987).

The $\varepsilon_{Hf}(t)$ values in the Loei rhyolites zircon grains are uniform and positive (4.03–5.38), which excludes the possibility of mingling of mantle-derived and crustal-derived magmas because it would produce a wide range of $\varepsilon_{Hf}(t)$ values. Besides, the hybrid melts of mantle mafic materials and crust felsic materials will result in elevated Mg# and low content of SiO_2, however, which is not seen in the studied rocks. On the other hand, the fractional crystallization of basaltic magmas is another model to explicate petrogenesis of highly fractionated I-type granites (Zhang et al., 2013; Wu et al., 2003a, b). Experiments have shown that mafic magmas can produce 12 wt.%–25 wt.% of granitoid magmas by differentiation (Sisson et al., 2005), suggesting that considerable basaltic materials would have been produced in the same area. However, no mafic or ultramafic rocks so far have been found or reported in the study area. In conclusion, the Loei rhyolites may have been produced by the partial melting of juvenile crust. Further, zircon Hf T_{2DM} (985 to 1 065 Ma) ages are older than zircon U-Pb age, suggesting the reworking of juvenile crustal sources and significant Neoproterozoic crustal growth. Neoproterozoic to Paleozoic is a main period for crustal formation of the Indochina Block (Lan et al., 2003), as well as assemblage of Gondwana (Cawood et al., 2013).

4.3 Tectonic Setting and Implications

The concentration of LILEs of the Loei rhyolite is high (such as Ba, K, Pb). They are relatively depleted in HFSEs (such as Th, Nb, Ta, Zr, Ti). These are main features of magmas formed in an active continental fringe related subduction setting (Qi et al., 2014). In the La/Yb versus Th/Yb tectonic discrimination diagram (Fig. 10b) (Condie, 1989), all the Loei rhyolites plot in the field of continental margin-arc. In a series of discrimination diagrams based on trace elements, most samples fall within the 'volcanic arc granitoid' (Figs. 10a, 10c, 10d) (Harris et al., 1986; Pearce et al., 1984). Enriched LREEs combined with negative Eu patterns are also the property of subduction-related granitoids (Peter and Silver, 1983). Therefore, these rocks may have formed in a subduction-related setting.

The Truong Son fold belt, located in central Vietnam and northeastern Laos, is one of the most important tectonic and metallogenic terranes in the Indochina Block. It presents a NW-SE trending elongated fold belt, and extends from the northern Song Ma suture, which defines the boundary between the Indochina and South China blocks, to the southern Tamky-Phuoc Son-Xepon (Laos) suture, which marks the boundary with the Kontum massif (Shi et al., 2015).

The Truong Son fold belt is in contact with Kontum massif which has experienced the same thermal and deformation history. Ordovician–Silurian (ca. 462–422 Ma) peraluminous granitoids which were metamorphosed in the Triassic are also reported in Kontum massif, suggesting the presence of the Ordovician–Silurian volcanic arc magmatism in the region (Nakano et al., 2013), metamorphism and felsic magmatism occurred at 430 Ma according to U-Pb dating of zircons and monazites, suggesting a regional subduction of ocean plate along the northeastern Gondwana margin (Tran et al., 2014). Granites from the Song Chay complex in northern Vietnam have zircon U-Pb age of 428±5 Ma (Roger et al., 2000). Moreover, significant volumes of arc-related mafic rocks occurred in northern and central Vietnam, they may represent a possible heat source for the Ordovician–Silurian low-P/T metamorphism (Nakano et al., 2013). The stratigraphical features of the Loei area are in good agreement with the regional geology of northern Vietnam and the Truong Son fold belt, where Pre-Devonian low-grade metasediments and unmetamorphic Devonian and younger sediments are separated by an angular unconformity, which is called "Caledonian" in the South China Block (Roger et al., 2000; Hutchison, 1989). Therefore, the Loei fold belt and the Truong Son fold belt contain widespread Silurian arc-related igneous rocks, suggesting that the Loei fold belt was in contact with the Truong Son fold belt. However, more study is needed for better understanding the extension of the Loei fold belt in Laos.

The Indochina Block was originated from eastern Gondwana and rifted since the Early Devonian (Lehmann et al., 2013; Metcalfe, 2013). The Silurian arc-related rhyolites in the western margin of the Indochina indicate that the arc developed in response to the subduction of Proto-Tethys oceanic plate underneath the Indochina Block before the opening of the Devonian Loei ocean (ca. 361 Ma) (Intasopa and Dunn, 1994). Lehmann et al. (2013) reported Mid-Silurian dacite volcanism and associated volcanic-hosted massive sulfide (VHMS) mineralization at Dapingzhang in the Lancangjiang zone of the Yunnan Province in South China. The Dapingzhang Mid-Silurian (429 Ma) dacite gave $\varepsilon_{Nd}(t)$ values of +2 to +5, suggesting a mantle sources (Lehmann et al., 2013), which is similar to Loei rhyolites. Moreover, The Late Silurian arc-related igneous rocks are present at the Dazhonghe in the western margin of Simao Block which also have postive $\varepsilon_{Nd}(t)$ values of 3.86 to 4.89. Therefore, we argue that the Simao Block may be contiguous with the Indochina Block during the Silurian. A similar conclusion was put forward previously by (Wang Y et al., 2014) based on detrital zircon data.

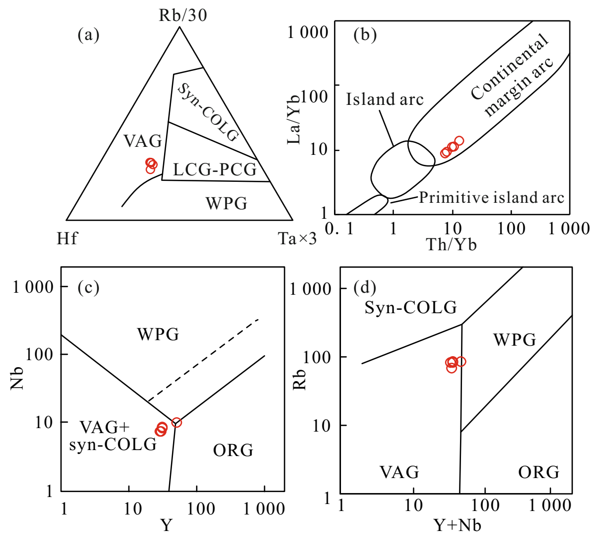

Figure 10. Discrimination diagrams of tectonic settings for the Loei rhyolite. (a) After Harris et al. (1986); (b) La/Yb vs. Th/Yb (after Condie, 1989); (c) Nb vs. Y and (d) Rb vs. Y+Nb (after Pearce et al., 1984). VAG. volcanic arc granites; Syn-COLG. syn-collisional granites; PCG. post-collisional granites; WPG. within plate granites; ORG. ocean ridge granites; LCG. late-collisional granites.

5 CONLUSIONS

(1) Zircon U-Pb ages indicate that the Loei rhyolites were erupted at 423.7±2.7 Ma.

(2) The Loei rhyolites are characterized by high SiO_2 and low P_2O_5. They are highly fractionated I-type rhyolites which were formed in an arc environment. They are the products of the reworking of juvenile crustal sources.

(3) The Simao Block may be contiguous with the Indochina Block during the Silurian. The Loei fold belt and the Truong Son fold belt contain widespread Silurian arc-related igneous rocks, suggesting that the Loei fold belt was in contact with the Truong Son fold belt during the Early Paleozoic.

ACKNOWLEDGMENTS

Two anonymous reviewers and editors are thanked for their constructive comments. This work was supported by the NSFC (Nos. 41172202 and 41190073), the China Geological Survey (No. 1212011121256), the Ministry of Education of China (No. 20110145130001), and the State Key Laboratory of Geological Processes and Mineral Resources, China University of Geosciences in Wuhan (No. MSFGPMR201402). The final publication is available at Springer via http://dx.doi.org/10.1007/s12583-016-0671-y.

REFERENCES CITED

Barr, S. M., Macdonald, A. S., Ounchanum P., et al., 2006. Age, Tectonic Setting and Regional Implications of the Chiang Khong Volcanic Suite, Northern Thailand. *Journal of the Geological Society*, 163(6): 1037–1046. doi:10.1144/0016-76492005-118

Boonsoong, A., Panjasawatwong, Y., Metparsopsan, K., 2011. Petrochemistry and Tectonic Setting of Mafic Volcanic Rocks in the Chon Daen-Wang Pong Area, Phetchabun, Thailand. *Island Arc*, 20(1): 107–124. doi:10.1111/j.1440-1738.2010.00748.x

Bunopas, S., Vella, P., 1983. Geological Society of Thailand and Geological Society of Malaysia. Tectonic and Geologic Evolution of Thailand Proceedings of the Workshop on Stratigraphic Correlation of Thailand and Malaysia, Haad Yai. 212–232

Burrett, C., Zaw, K., Meffre S., et al., 2014. The Configuration of Greater Gondwana–Evidence from LA-ICPMS, U-Pb Geochronology of Detrital Zircons from the Palaeozoic and Mesozoic of Southeast Asia and China. *Gondwana Research*, 26(1SI): 31–51. doi:10.1016/j.gr.2013.05.020

Cawood, P. A., Wang, Y. J., Xu, Y. J., et al., 2013. Locating South China in Rodinia and Gondwana: A Fragment of Greater India Lithosphere? *Geology*, 41(8): 903–906. doi:10.1130/G34395.1

Chappell, B. W., 1999. Aluminium Saturation in I- and S-Type Granites and the Characterization of Fractionated Haplogranites. *Lithos*, 46(3): 535–551. doi:10.1016/S0024-4937(98)00086-3

Charoenprawat, A., Wongwanich, T., Tantiwanit, W., et al., 1976. Geological Map of Thailand 1 : 250 000 Sheet Changwat Loei. Department of Mineral Resources, Bangkok

Chonglakmani, C., Helmcke, D., 2001. Geodynamic Evolution of Loei and Phetchabun Regions—Does the Discovery of Detrital Chromian Spinels from the Nam Duk Formation (Permian, North-Central Thailand) Provide New Constraint? *Gondwana Research*, 4(3): 437–442. doi:10.1016/S1342-937X(05)70343-9

Condie, K. C., 1989. Geochemical Changes in Baslts and Andesites across the ArcheanProterozoic Boundary: Identification and Significance. *Lithos*, 23(1/2): 1–18. doi:10.1016/0024-4937(89)90020-0

Dong, M. L., Dong, G. C., Mo, X. X., et al., 2013. Geochemistry, Zircon U-Pb Geochronology and Hf Isotopes of Granites in the Baoshan Block, Western Yunnan: Implications for Early Paleozoic Evolution along the Gondwana Margin. *Lithos*, 179: 36–47. doi:10.1016/j.lithos.2013.05.011

Feng, Q. L., Chonglakmani, C., Helmcke, D., et al., 2005. Correlation of Triassic Stratigraphy between the Simao and Lampang-Phrae Basins: Implications for the Tectonopaleogeography of Southeast Asia. *Journal of Asian Earth Sciences*, 24(6): 777–785. doi:10.1016/j.jseaes.2004.11.008

Gong, S. L., Chen, N. S., Geng, H. Y., et al., 2014. Zircon Hf Isotopes and Geochemistry of the Early Paleoproterozoic High-Sr Low-Y Quartz-Diorite in the Quanji Massif, NW China: Crustal Growth and Tectonic Implications. *Journal of Earth Science*, 25(1): 74–86. doi:10.1007/s12583-014-0401-2

Harris, N. B. W., Pearce, J. A., Tindle, A. G., 1986. Geochemical Characteristics of Collision-Zone Magmatism. *Geological Society*, *London*, *Special Publications*, 19(1): 67–81. doi:10.1144/GSL.SP.1986.019.01.04

Hoskin, P. W., Schaltegger, U., 2003. The Composition of Zircon and Igneous and Metamorphic Petrogenesis. *Reviews in Mineralogy and Geochemistry*, 53(1): 27–62. doi:10.2113/0530027

Hu, Z. C., Liu, Y. S., Gao, S., et al., 2012. Improved In Situ Hf Isotope Ratio Analysis of Zircon Using Newly Designed *X* Skimmer Cone and Jet Sample Cone in Combination with the Addition of Nitrogen by Laser Ablation Multiple Collector ICP-MS. *Journal of Analytical Atomic Spectrometry*, 27(9): 1391–1399. doi:0.1039/C2JA30078H

Hutchison, C. S., 1989. Geological Evolution of South-East Asia. Clarendon Press, Oxford

Intasopa, S., Dunn, T., 1994. Petrology and Sr-Nd Isotopic Systems of the Basalts and Rhyolites, Loei, Thailand. *Journal of Southeast Asian Earth Sciences*, 9(1): 167–180. doi:10.1016/0743-9547(94)90073-6

Irvine, T., Baragar, W., 1971. A Guide to the Chemical Classification of the Common Volcanic Rocks. *Canadian Journal of Earth Sciences*, 8(5): 523–548. doi:10.1139/e71-055

Ji, W. Q., Wu, F. Y., Chung, S. L., et al., 2009. Zircon U-Pb Geochronology and Hf Isotopic Constraints on Petrogenesis of the Gangdese Batholith, Southern Tibet. *Chemical Geology*, 262(3/4): 229–245. doi:10.1016/j.chemgeo.2009.01.020

Jungyusuk, N., Khositanont, S, 1992. Volcanic Rocks and Associated Mineralization in Thailand. In: Piencharoen, C., ed., Proceedings of the National Conference on Geologic Resources of Thailand: Potential for Future Development, Department of Mineral Resources, Bangkok. 528–532

Kamvong, T., Zaw, K., Meffre, S., et al., 2014. Adakites in the Truong Son and Loei Fold Belts, Thailand and Laos: Genesis and Implications for Geodynamics and Metallogeny. *Gondwana Research*, 26(1): 165–184. doi:10.1016/j.gr.2013.06.011

Kelemen, P. B., Hanghøj, K., Greene, A. R., 2003. One View of the Geochemistry of Subduction-Related Magmatic Arcs, with an Emphasis on Primitive Andesite and Lower Crust. *Treatise on Geochemistry*, 3: 593–659. doi:10.1016/B0-08-043751-6/03035-8

Khositanont, S., Panjasawatwong, Y., Ounchanum, P., et al., 2008. Petrochemistry and Zircon Age Determination of Loei-Phetchabun Volcanic Rocks. Proceedings of the International Symposia on Geoscience Resources and Environments of Asian Terranes (GREAT 2008), Bangkok. 272–280

Kinny, P. D., Maas, R., 2003. Lu-Hf and Sm-Nd Isotope Systems in Zircon. *Reviews in Mineralogy and Geochemistry*, 53(1): 327–341. doi:10.2113/0530327

Lan, C. Y., Chung, S. L., Van Long, T., et al., 2003. Geochemical and Sr-Nd Isotopic Constraints from the Kontum Massif, Central Vietnam on the Crustal Evolution of the Indochina Block. *Precambrian Research*, 122(1): 7–27. doi:10.1016/S0301-9268(02)00205-X

Le Bas, M. J., Le Maitre, R. W., Streckeisen, A., et al., 1986. A Chemical Classification of Volcanic Rocks Based on the Total Alkali-Silica Diagram. *Journal of Petrology*, 27(3): 745–750. doi:10.1093/petrology/27.3.745

Lehmann, B., Zhao, X. F., Zhou, M. F., et al., 2013. Mid-Silurian Back-Arc Spreading at the Northeastern Margin of Gondwana: The Dapingzhang Dacite-Hosted Massive Sulfide Deposit, Lancangjiang Zone, Southwestern Yunnan, China. *Gondwana Research*, 24(2): 648–663. doi:10.1016/j.gr.2012.12.018

Li, X. H., Li, Z. X., Li, W. X., et al., 2007. U-Pb Zircon, Geochemical and Sr-Nd-Hf Isotopic Constraints on Age and Origin of Jurassic I- and A-Type Granites from Central Guangdong, SE China: A Major Igneous Event in Response to Foundering of a Subducted Flat-Slab? *Lithos*, 96(1/2): 186–204. doi:10.1016/j.lithos.2006.09.018

Liu, H. C., Wang Y. J., Fan W. M., et al., 2014. Petrogenesis and Tectonic Implications of Late-Triassic High $\varepsilon_{Nd}(t)$-$\varepsilon_{Hf}(t)$ Granites in the Ailaoshan Tectonic Zone (SW China). *Science China*: *Earth Sciences*, 57(9): 2181–2194. doi:10.1007/s11430-014-4854-z

Liu, Y. S., Gao, S., Hu, Z. C., et al., 2009. Continental and Oceanic Crust Recycling-Induced Melt-Peridotite Interactions in the Trans-North China Orogen: U-Pb Dating, Hf Isotopes and Trace Elements in Zircons from Mantle Xenoliths. *Journal of Petrology*, 51(1/2): 537–571, doi:10.1093/petrology/egp082

Liu, Y. S., Hu, Z. C., Zong, K. Q., et al., 2010. Reappraisement and Refinement of Zircon U-Pb Isotope and Trace Element Analyses by LA-ICP-MS. *Chinese Science Bulletin*, 55(15): 1535–1546. doi:10.1007/s11434-010-3052-4

Liu, Y. S., Zong, K. Q., Kelemen, P. B., et al., 2008. Geochemistry and Magmatic History of Eclogites and Ultramafic Rocks from the Chinese Continental Scientific Drill Hole: Subduction and Ultrahigh-Pressure Metamorphism of Lower Crustal Cumulates. *Chemical Geology*, 247(1): 133–153. doi:10.1016/j.chemgeo.2007.10.016

Ludwig, K. R., 2003. User's Manual for Isoplot 3.00: A Geochronological Toolkit for Microsoft Excel. Berkeley Geochronology Center Special Publication, Berkeley. 1–74

Maniar, P. D., Piccoli, P. M., 1989. Tectonic Discrimination of Granitoids. *Geological Society of America Bulletin*, 101(5): 635–643. doi:10.1130/0016-7606(1989)101<0635:TDOG> 2.3.CO;2

Mao, X. C., Wang, L. Q., Li, B., et al., 2012. Discovery of the Late Silurian Volcanic Rocks in the Dazhonghe Area, Yunxian-Jinggu Volcanic Arcbelt, Western Yunnan, China and Its Geological Significance. *Acta Petrologica Sinica*, 28(5): 1517–1528 (in Chinese with English Abstract)

Metcalfe, I., 2013. Gondwana Dispersion and Asian Accretion: Tectonic and Palaeogeographic Evolution of Eastern Tethys. *Journal of Asian Earth Sciences*, 66: 1–33. doi:10.1016/j.jseaes.2012.12.020

Nagy, E. A., Maluski, H., Lepvrier, C., et al., 2001. Geodynamic Significance of the Kontum Massif in Central Vietnam: Composite $^{40}Ar/^{39}Ar$ and U-Pb Ages from Paleozoic to Triassic. *The Journal of Geology*, 109: 755–770. doi:10.1086/323193

Nakano, N., Osanai, Y., Owada, M., et al., 2013. Tectonic Evolution of High-Grade Metamorphic Terranes in Central Vietnam: Constraints from Large-Scale Monazite Geochronology. *Journal of Asian Earth Sciences*, 73: 520–539. doi:10.1016/j.jseaes.2013.05.010

Panjasawatwong, Y., Zaw, K., Chantaramee, S., et al., 2006. Geochemistry and Tectonic Setting of the Central Loei Volcanic Rocks, Pak Chom Area, Loei, Northeastern Thailand. *Journal of Asian Earth Sciences*, 26(1): 77–90. doi:10.1016/j.jseaes.2004.09.008

Pearce, J. A., Harris, N. B., Tindle, A. G., 1984. Trace Element Discrimination Diagrams for the Tectonic Interpretation of Granitic Rocks. *Journal of Petrology*, 25(4): 956–983. doi:10.1093/petrology/25.4.956

Peter, G. L., Silver, L. T., 1983. Rare Earth Element Distributions among Minerals in a Granodiorite and Their Petrogenetic Implications. *Geochimica et Cosmochimica Acta*, 47(5): 925–939. doi:10.1016/0016-7037(83)90158-8

Qi, X. X., Santosh, M., Zhu, L. H., et al., 2014. Mid-Neoproterozoic Arc Margin of the Indochina Block, SW China: Geochronological and Petrogenetic Constraints and Implications for Gondwana Assembly. *Precambrian Research*, 245: 207–224. doi:10.1016/j.precamres.2014.02.008

Qian, X., Feng, Q. L., Chonglakmani, C., et al., 2013. Geochemical and Geochronological Constrains on the Chiang Khong Volcanic Rocks (Northwestern Thailand) and Its Tectonic Implications. *Frontiers of Earth Science*, 7(4): 508–521. doi:10.1007/s11707-013-0399-2

Qian, X., Feng, Q. L., Wang Y. J., et al., 2015. Arc-Like Volcanic Rocks in NW Laos: Geochronological and Geochemical Constraints and Their Tectonic Implications.

Journal of Asian Earth Sciences, 98: 342–357. doi:10.1016/j.jseaes.2014.11.035

Roger, F., Leloup, P. H., Jolivet, M., et al., 2000. Long and Complex Thermal History of the Song Chay Metamorphic Dome (Northern Vietnam) by Multi-System Geochronology. *Tectonophysics*, 321(4): 449–466. doi:10.1016/S0040-1951(00)00085-8

Salam, A., Zaw, K., Meffre, S., et al., 2014. Geochemistry and Geochronology of the Chatree Epithermal Gold-Silver Deposit: Implications for the Tectonic Setting of the Loei Fold Belt, Central Thailand. *Gondwana Research*, 26(1): 198–217. doi:10.1016/j.gr.2013.10.008

Shi, M. F., Lin, F. C., Fan, W. Y., et al., 2015. Zircon U-Pb Ages and Geochemistry of Granitoids in the Truong Son Terrane, Vietnam: Tectonic and Metallogenic Implications. *Journal of Asian Earth Sciences*, 101: 101–120. doi:10.1016/j.jseaes.2015.02.001

Sisson, T. W., Ratajeski, K., Hankins, W. B., et al., 2005. Voluminous Granitic Magmas from Common Basaltic Sources. *Contributions to Mineralogy and Petrology*, 148(6): 635–661. doi:10.1007/s00410-004-0632-9

Sun, S. S., McDonough, W. F., 1989. Chemical and Isotopic Systematics of Oceanic Basalts: Implications for Mantle Composition and Processes. *Geological Society*, *London*, *Special Publications*, 42(1): 313–345. doi:10.1144/GSL.SP.1989.042.01.19

Sylvester, P. J., 1998. Post-Collisional Strongly Peraluminous Granites. *Litho*s, 45(1): 29–44. doi:10.1016/S0024-4937(98)00024-3

Tao, J. H., Li, W. X., Li, X. H., et al., 2013. Petrogenesis of Early Yanshanian Highly Evolved Granites in the Longyuanba Area, Southern Jiangxi Province: Evidence from Zircon U-Pb Dating, Hf-O Isotope and Whole-Rock Geochemistry. *Science China Earth Sciences*, 56(6): 922–939. doi:10.1007/s11430-013-4593-6

Tran, H. T., Zaw, K., Halpin, J. A., et al., 2014. The Tam Ky-Phuoc Son Shear Zone in Central Vietnam: Tectonic and Metallogenic Implications. *Gondwana Research*, 26(1): 144–146. doi:10.1016/j.gr.2013.04.008

Udchachon, M., Thassanapak, H., Feng, Q. L., et al., 2011. Geochemical Constraints on the Depositional Environment of Upper Devonian Radiolarian Cherts from Loei, North-Eastern Thailand. *Frontiers of Earth Science*, 5(2): 178–190. doi:10.1007/s11707-011-0153-6

Vivatpinyo, J., Charusiri, P., Sutthirat, C., 2014. Volcanic Rocks from Q-Prospect, Chatree Gold Deposit, Phichit Province, North Central Thailand: Indicators of Ancient Subduction. *Arabian Journal for Science and Engineering*, 39(1): 325–338. doi:10.1007/s13369-013-0839-z

Wang, Q. F., Deng, J., Li, C., et al., 2014. The Boundary between the Simao and Yangtze Blocks and Their Locations in Gondwana and Rodinia: Constraints from Detrital and Inherited Zircons. *Gondwana Research*, 26(2): 438–448. doi:10.1016/j.gr.2013.10.002

Wang, Y., Zhang, Y., Fan, W., et al., 2014. Early Neoproterozoic Accretionary Assemblage in the Cathaysia Block: Geochronological, Lu-Hf Isotopic and Geochemical Evidence from Granitoid Gneisses. *Precambrian Research*, 249: 144–161

Whalen, J. B., Currie, K. L., Chappell, B. W., 1987. A-Type Granites: Geochemical Characteristics, Discrimination and Petrogenesis. *Contributions to Mineralogy and Petrology*, 95(4): 407–419. doi:10.1007/BF00402202

Winchester, J. A., Floyd, P. A., 1977. Geochemical Discrimination of Different Magma Series and Their Differentiation Products Using Immobile Elements. *Chemical Geology*, 20: 325–343. doi:10.1016/0009-2541(77)90057-2

Wu, F. Y., Jahn, B., Wilde, S. A., et al., 2003a. Highly Fractionated I-Type Granites in NE China (I): Geochronology and Petrogenesis. *Lithos*, 66(3): 241–273. doi:10.1016/S0024-4937(02)00222-0

Wu, F. Y., Jahn, B., Wilde, S. A., et al., 2003b. Highly Fractionated I-Type Granites in NE China (II): Isotopic Geochemistry and Implications for Crustal Growth in the Phanerozoic. *Lithos*, 67(3/4): 191–204. doi:10.1016/S0024-4937(03)00015-X

Zhang, D. H., Wei, J. H., Fu, L. B., et al., 2013. Formation of the Jurassic Changboshan-Xieniqishan Highly Fractionated I-Type Granites, Northeastern China: Implication for the Partial Melting of Juvenile Crust Induced by Asthenospheric Mantle Upwelling. *Geological Journal*, 50(2): 122–138. doi:10.1002/gj.2531

Zhao, S., Xu, W. L., Wang, W., et al., 2014. Geochronology and Geochemistry of Middle-Late Ordovician Granites and Gabbros in the Erguna Region, NE China: Implications for the Tectonic Evolution of the Erguna Massif. *Journal of Earth Science*, 25(5): 841–853. doi: 10.1007/s12583-014-0476-9

Zhu, D. C., Zhao, Z. D., Niu, Y. L., et al., 2012. Cambrian Bimodal Volcanism in the Lhasa Terrane, Southern Tibet: Record of an Early Paleozoic Andean-Type Magmatic Arc in the Australian Proto-Tethyan Margin. *Chemical Geology*, 328: 290–308. doi:10.1016/j.chemgeo.2011.12.024